Observational probes of reionization

i. CMB Polarization.
ii. Lyman-α forest data.
iii. Opacity of ionizing photons.
iv. Temperature evolution.
v. HST WPC3 results
vi. Soft Xray BG
vii. IR BG (HESS results)

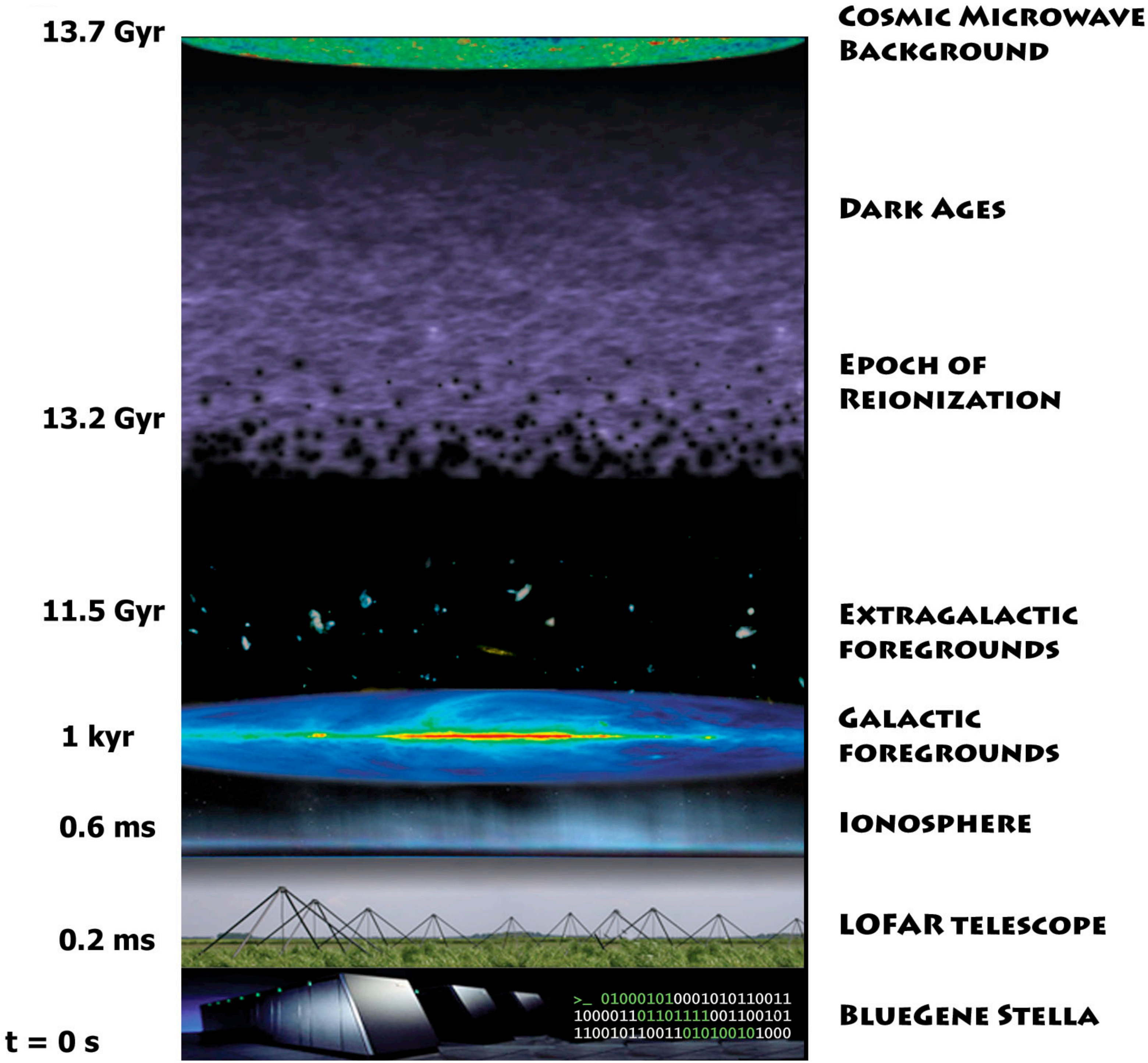
13.7 Gyr
13.2 Gyr
11.5 Gyr
1 kyr
0.6 ms
0.2 ms
t = 0 s
Cosmic Microwave Background
Dark Ages
Epoch of Reionization
Extragalactic foregrounds
Galactic foregrounds
Ionosphere
LOFAR telescope
BlueGene Stella
>_ 01000101000101010110011
100001101101111001100101
1100101100110101001011000

Key Probes of Reionization

- CMB (integral constraint)
- Redshifted 21 cm emission (absorption)
- 21 cm forest at high z
- Gamma ray bursts: How many we should have to constrain reionization?
- Luminosity function of first objects, e.g., Galaxies: Recent results from the new WFC3 aboard HST.
- Background detections: IR, soft x-ray.
- Lyman-α absorption system: ionization, metallicity, thermal history, UV background, proximity effect.
- Lyman alpha emitters
- Metals at high redshift.
- Using the local volume to study reionization.

CMB and Reionization

- Influence of reionization on CMB Temperature fluctuations
- Influence of reionization on CMB polarization.

References:

1. Scott, White & Silk 1994 (review).
2. Hu & White 1997
3. Aghanim,Subhabrata & Silk 2008 (review)
4. WMAP papers.

CMB photons Thomson scatter off free electrons

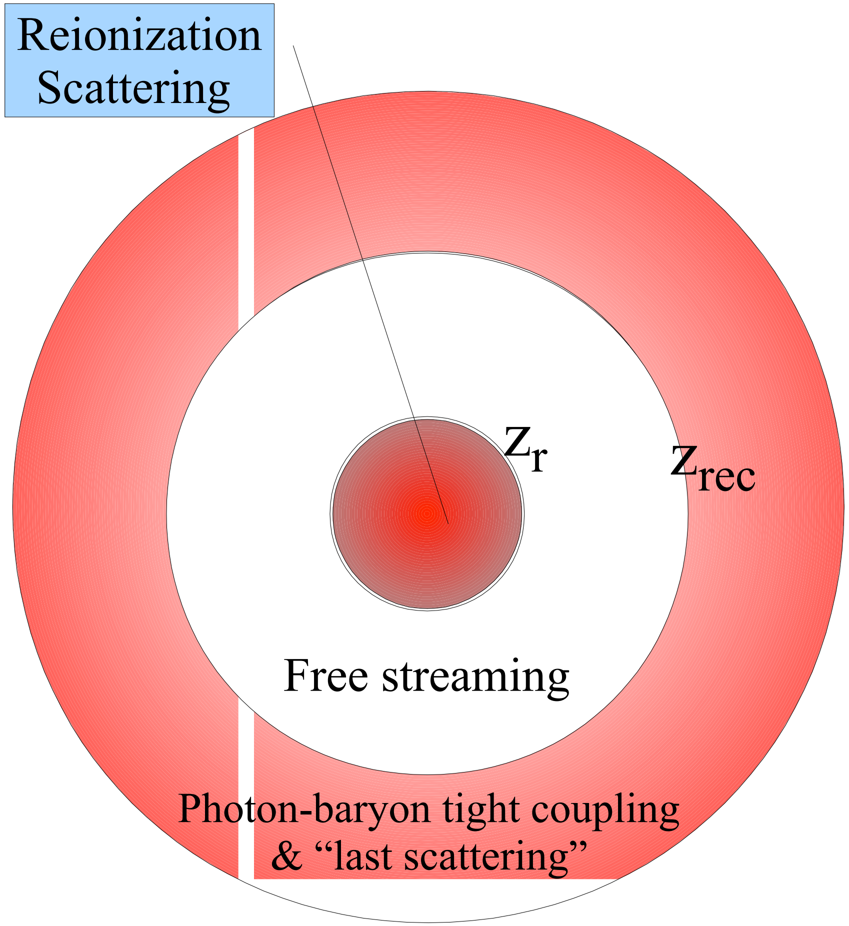

The dominant contribution to temperature anisotropies generated during reionization are Doppler shifts of the scatterers

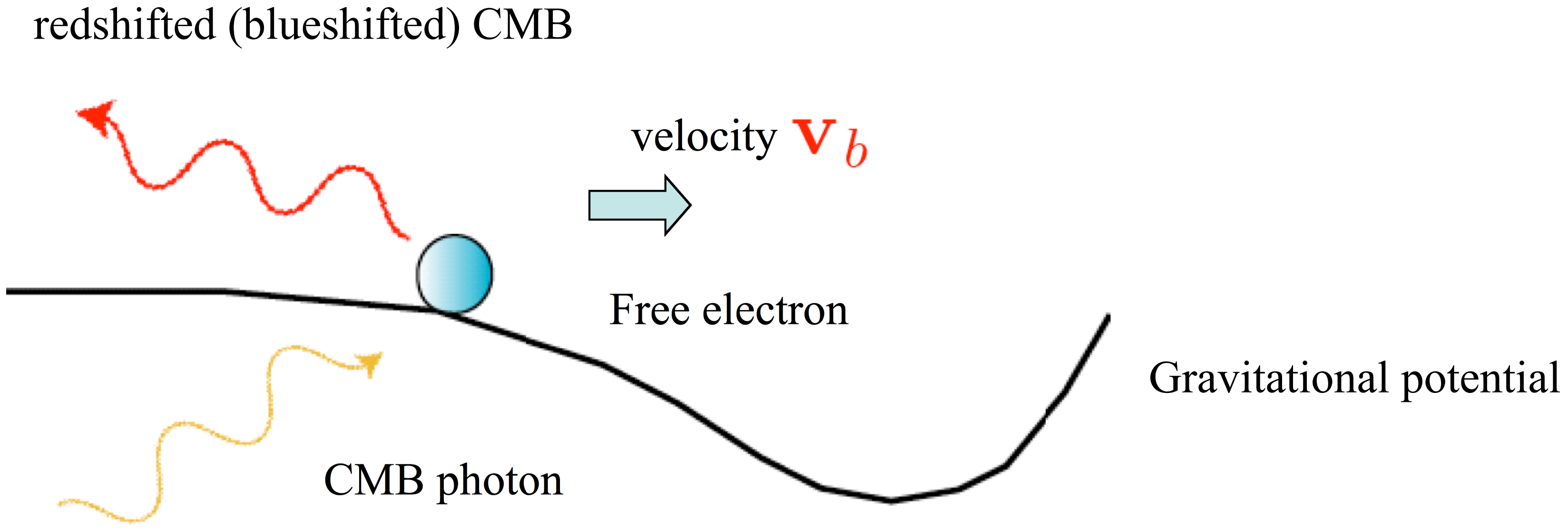

$$T_D(\hat{\mathbf{n}}) = -T_{\mathrm{cmb}} \int_0^{\eta_0} d\eta\, g(\eta)\, \hat{\mathbf{n}} \cdot \mathbf{v}_b(\hat{\mathbf{n}}, \eta)$$

$$g(\eta) = \dot{\tau} e^{-\tau}, \ \dot{\tau} = x_e n_b \sigma_T$$

The CMB and Reionization: Temperature

- Imprint on CMB anisotropies governed by the visibility – or probability that a photon scatters out of the line of sight:

$$g = \dot{\tau} e^{-\tau}$$

- τ is the optical depth given by

$$\dot{\tau} = x_e n_H \sigma_T$$

with $x_e n_H$ the number density of free electrons

Reionization & CMB Temperature

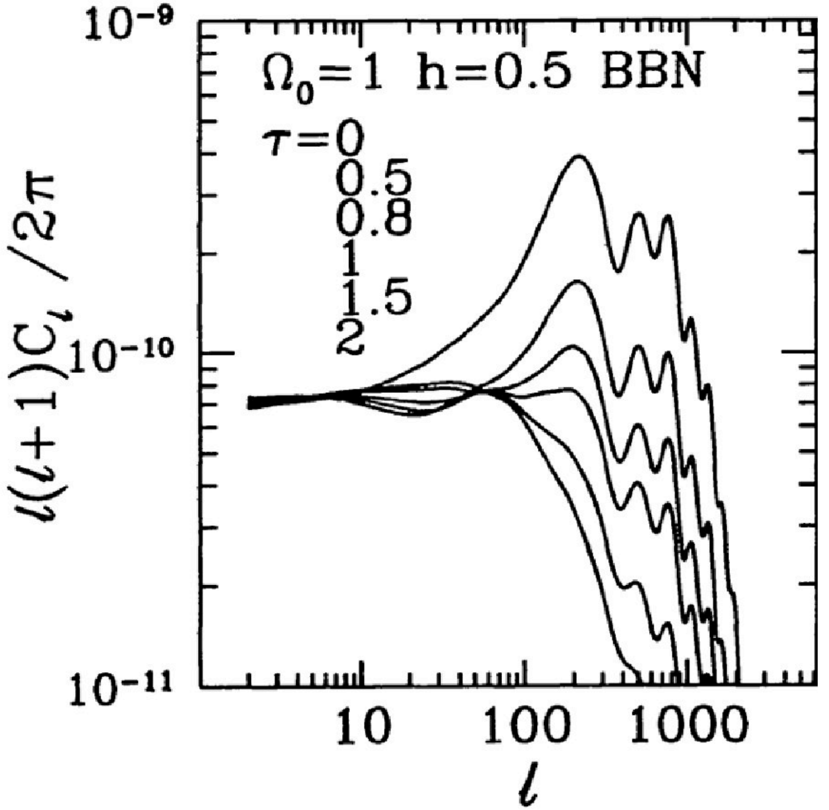

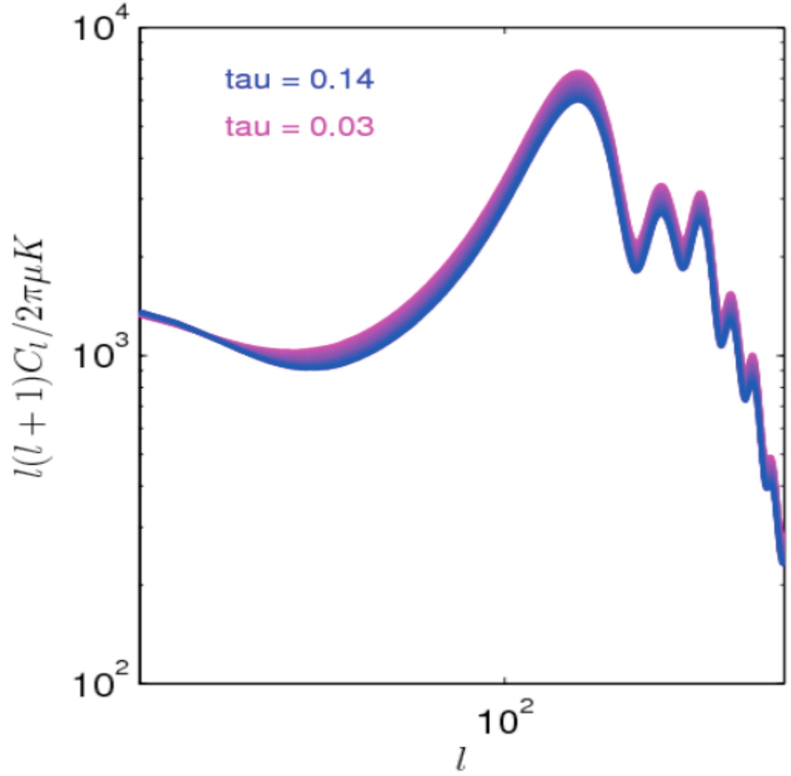

The influence of reionization on the CMB temperature angular power spectrum. (from Sugiyama 1995)

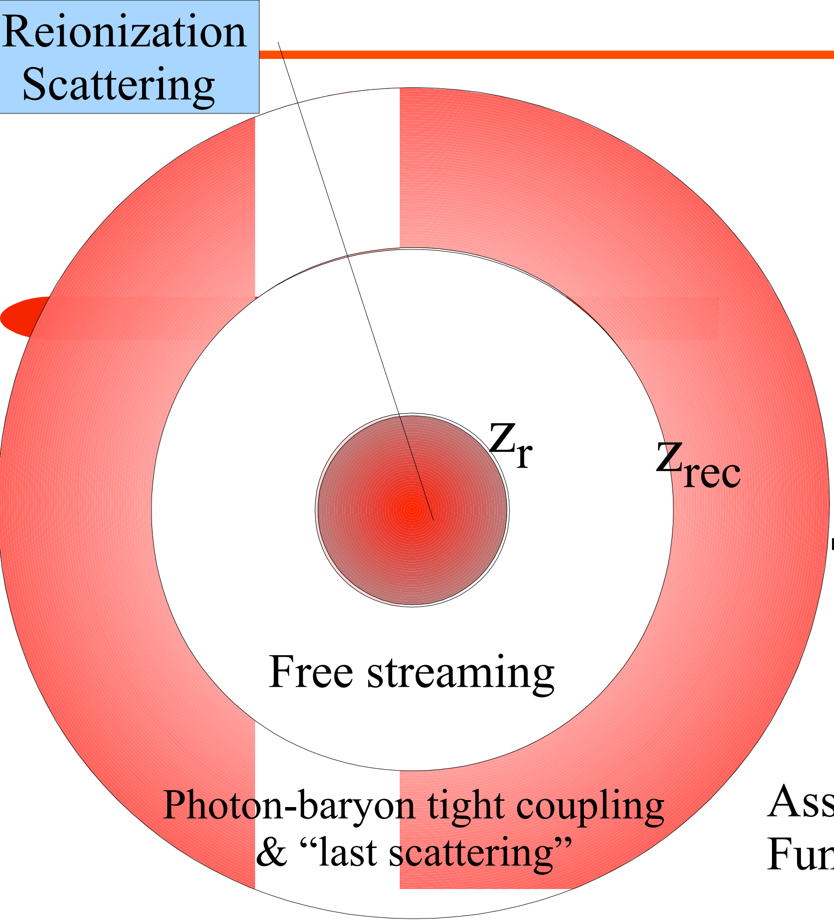

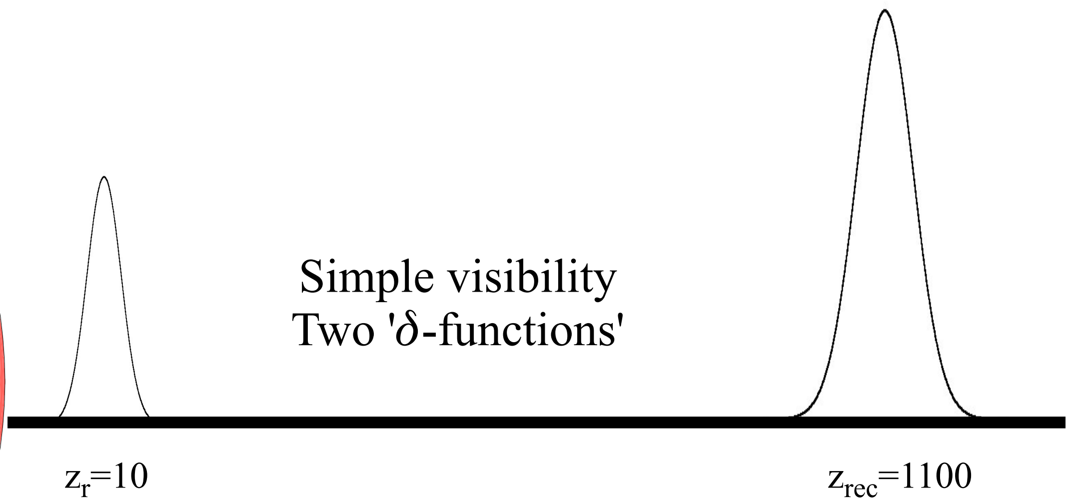

Assuming that the visibility is given by two delta Functions, the CMB is given by the following expression:

$$\Delta_l = e^{-\tau(z_r)} F_l(z_{rec}) + \left[1 - e^{-\tau(z_r)}\right] F_l(z_r) + ISW + \ldots$$

For the astrophysical reionization scenarios (low optical depth) second term negligible

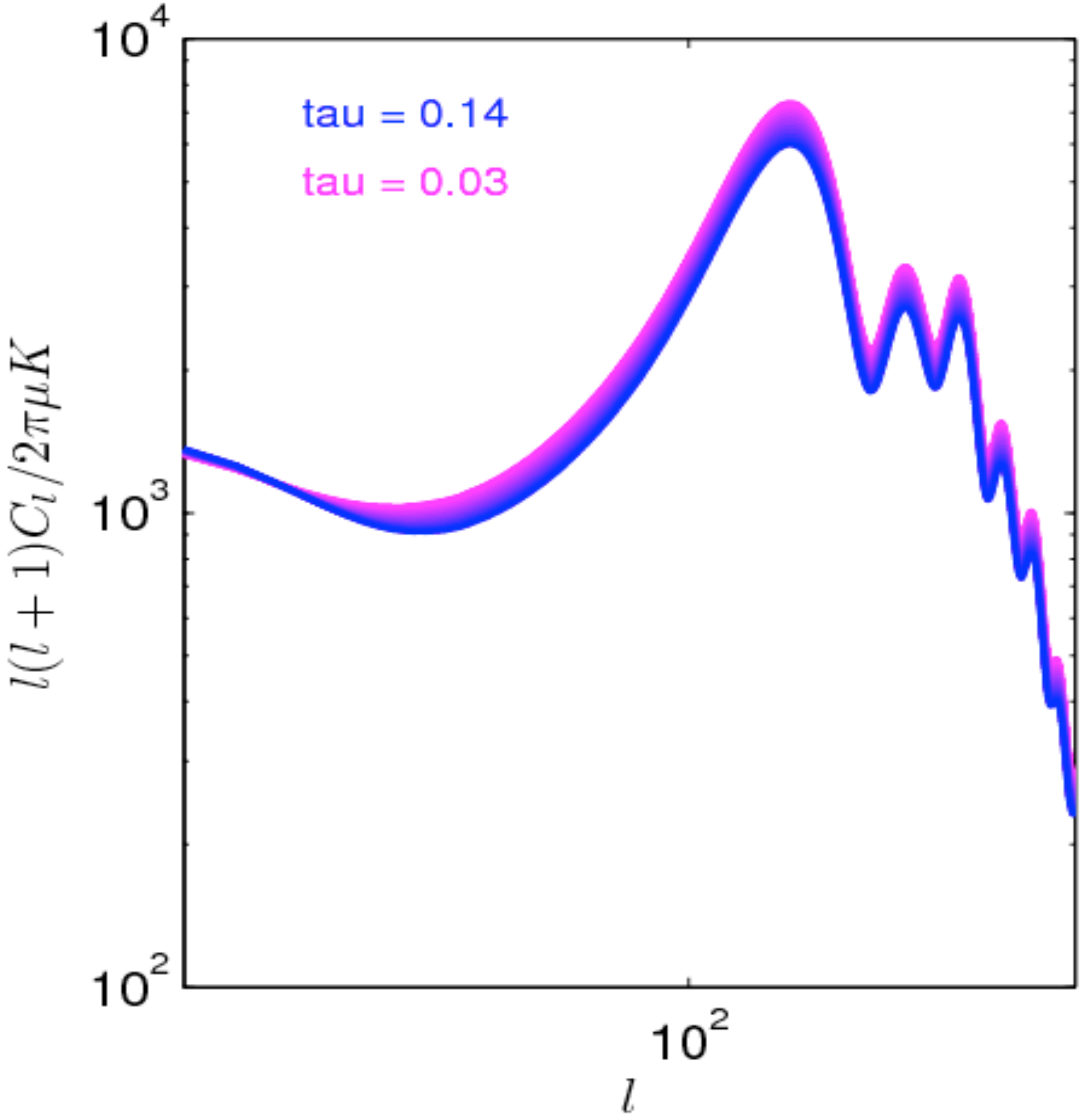

From A. Lewis

CMB and Reionization: Polarization

Polarization: Stokes parameters

Q → -Q, U → -U under 90 degree rotation
Q → U, U → -Q under 45 degree rotation

$$P = \sqrt{Q^2 + U^2} \quad \text{and} \quad \alpha = \frac{1}{2}\arctan(U/Q).$$

amplitude angle

Thomson scattering

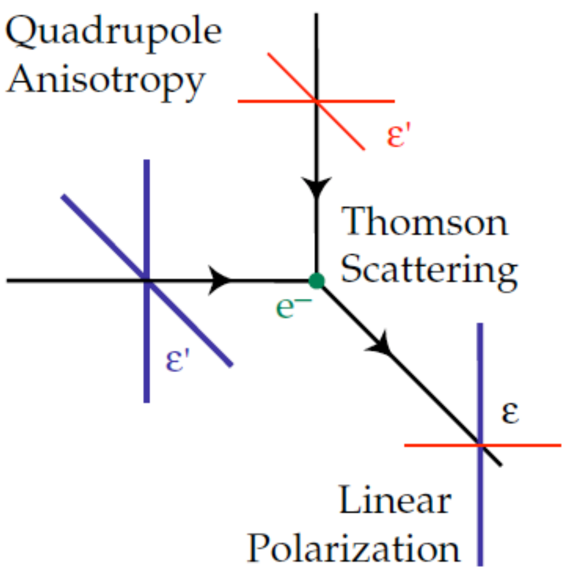

Q and U are generated by Thomson scattering of unpolarized light. Notice no V (circular polarization) is generated.

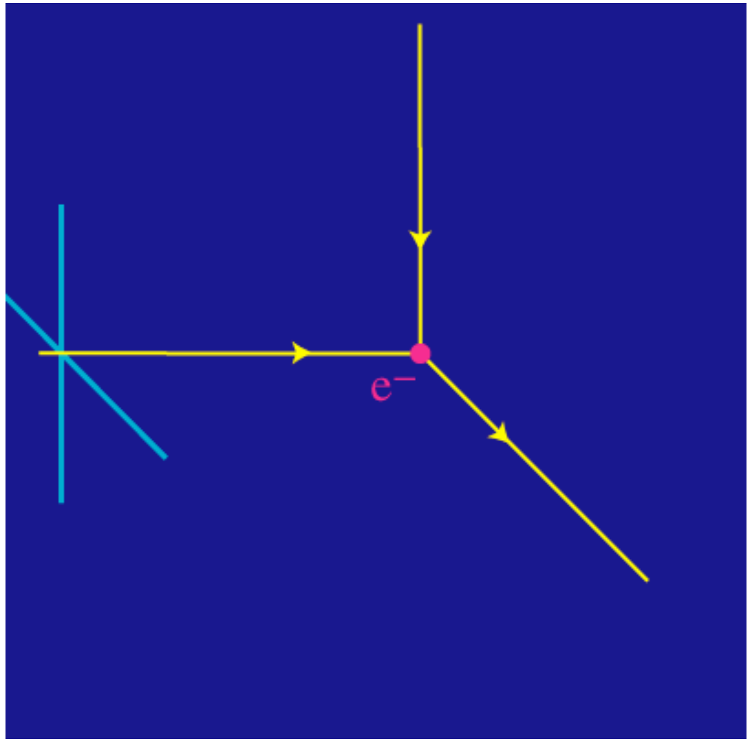

$$\frac{d\sigma_T}{d\Omega} = \frac{e^4}{m_e^2 c^4} |\vec{\epsilon} \cdot \vec{\epsilon}'|^2$$

E and B polarization modes

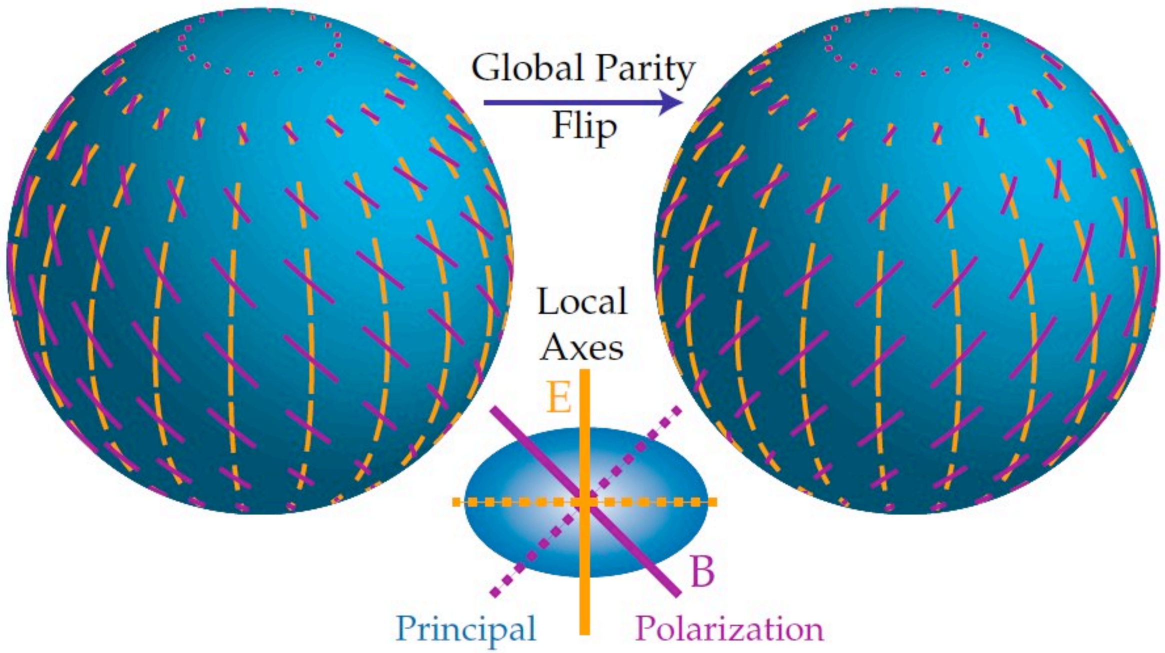

E-mode has $(-1)^{l}$ parity whereas B-mode $(-1)^{l+1}$

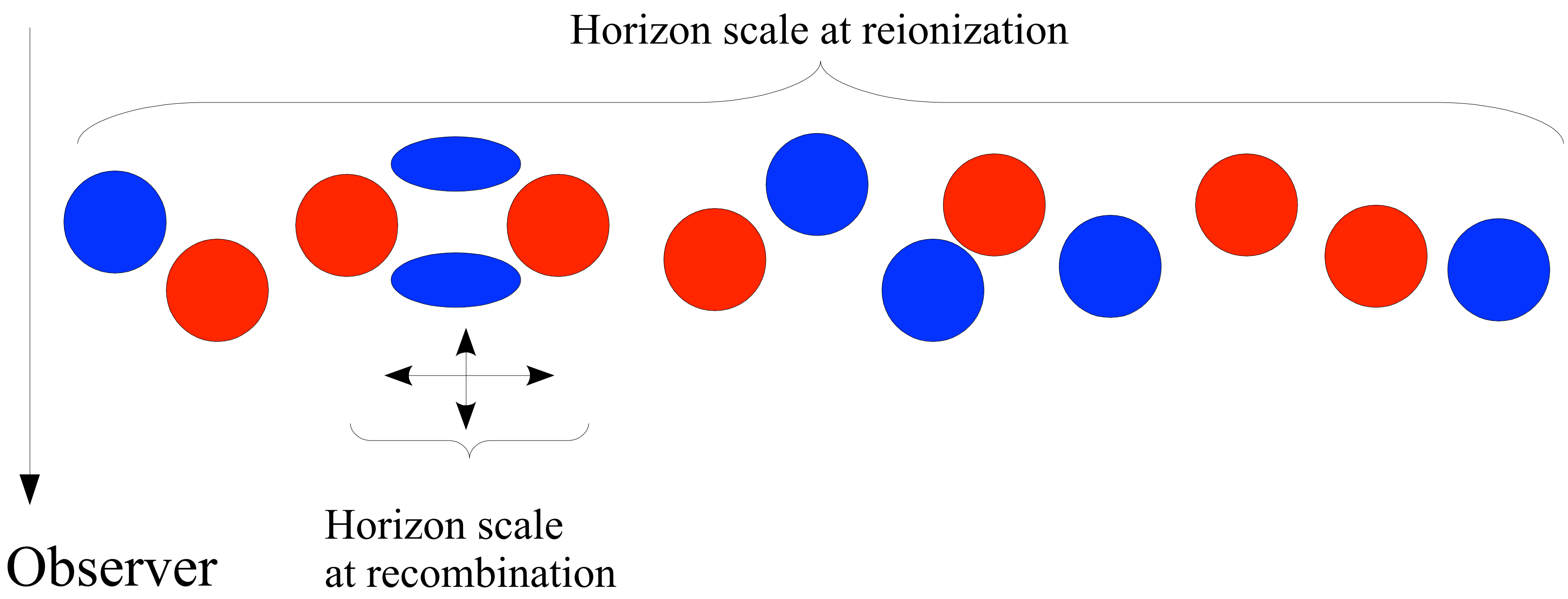

Given the geometry of linear polarization the amplitude of the signal at any scale depends on the local quadrupole that scatters the photons. However, at scales larger than horizon scales (either at recombination or during reionization) there is no coherence and the signal decays.

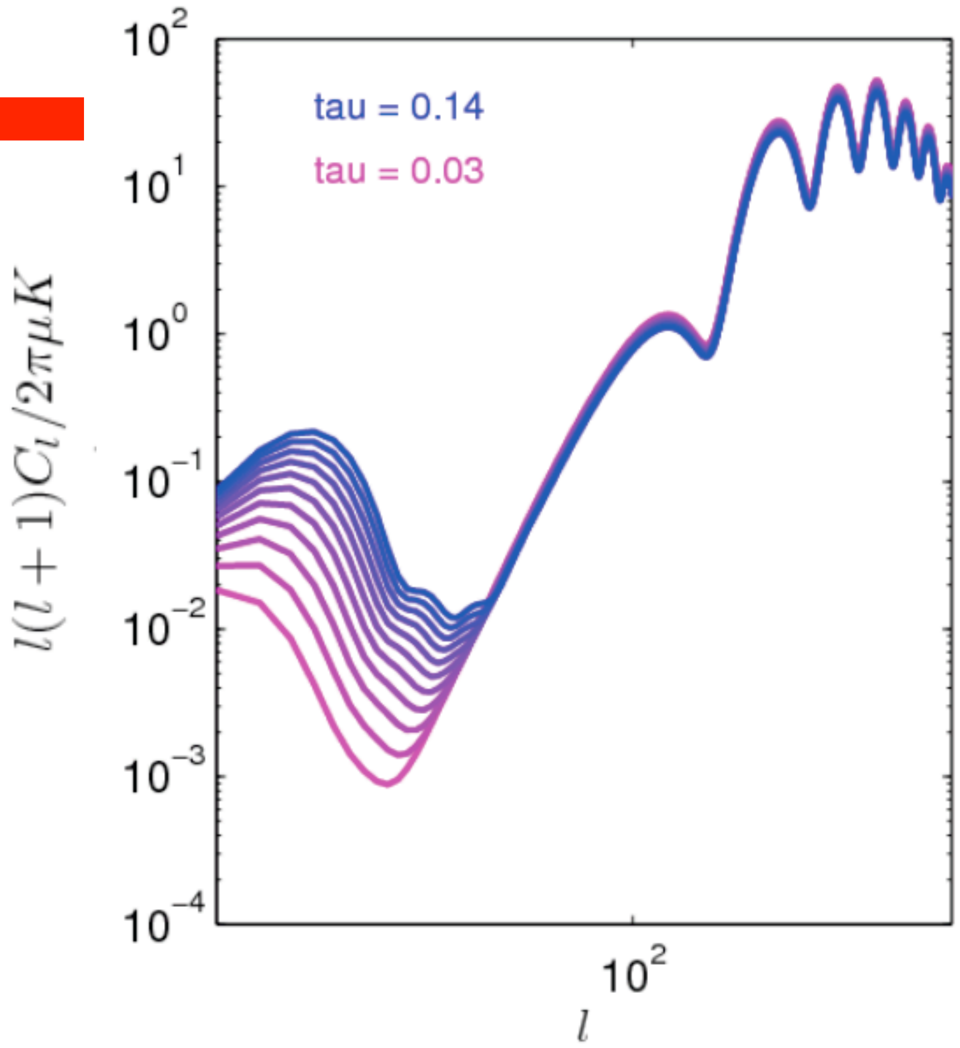

The influence of reionization is shown on the large scale amplitude and shape of the E-mode polarization power spectrum.

From A. Lewis

The WMAP cosntraint

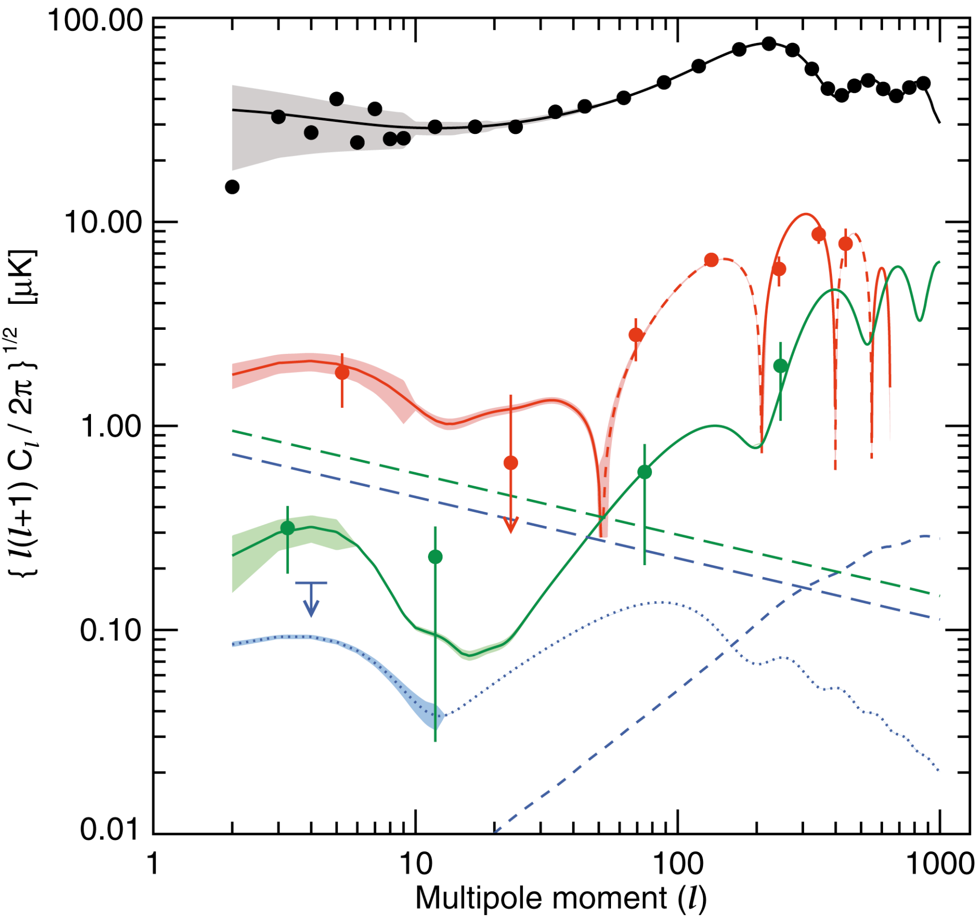

$\tau \sim 0.088$

- The WMAP polarization measurement tells us only about the optical depth not about exact ionization redshift. For that one needs a reionization history model. However, reasonable reionization models suggest that ionization has happened at about $z \sim 10$.

Sudden reionization ....

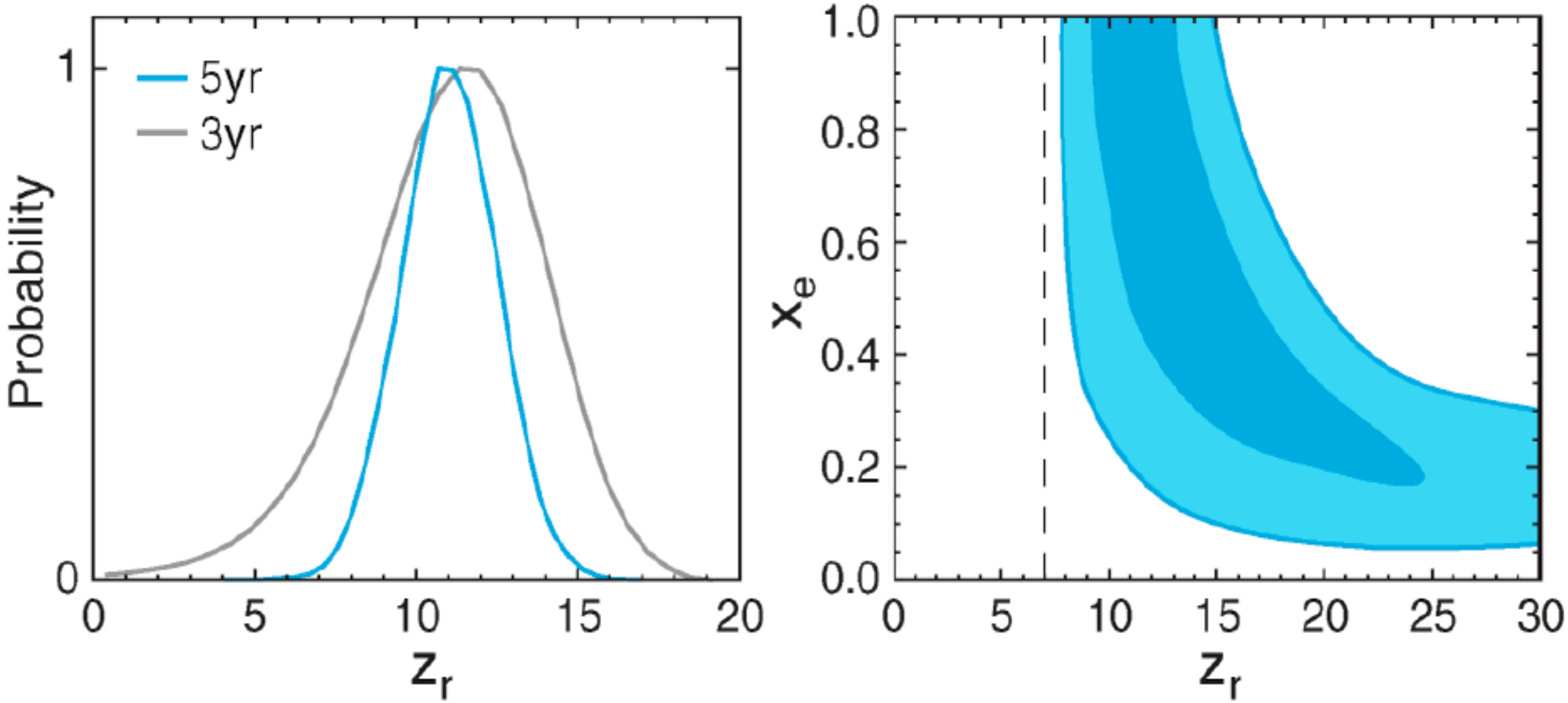

The Lyman-α optical depth from Quasar spectra

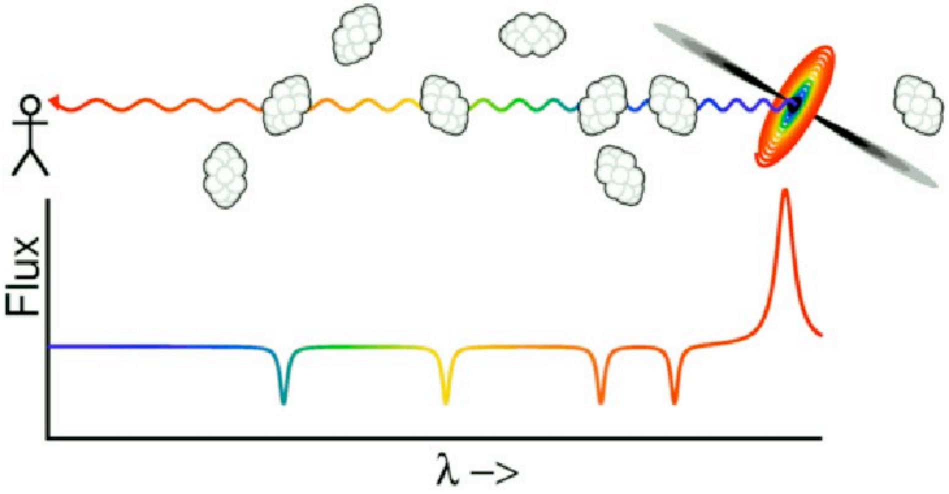

Absorption features due to Lyman-α in the IGM.

$$\tau_\alpha(\nu_0) = \int_{x_A}^{x_B} n_{HI}\sigma_\alpha dx/(1+z)$$

τ_α is the optical depth.x is the comoving radial distance. σ_α is the cross section & n_{HI} is the neutral hydrogen number density

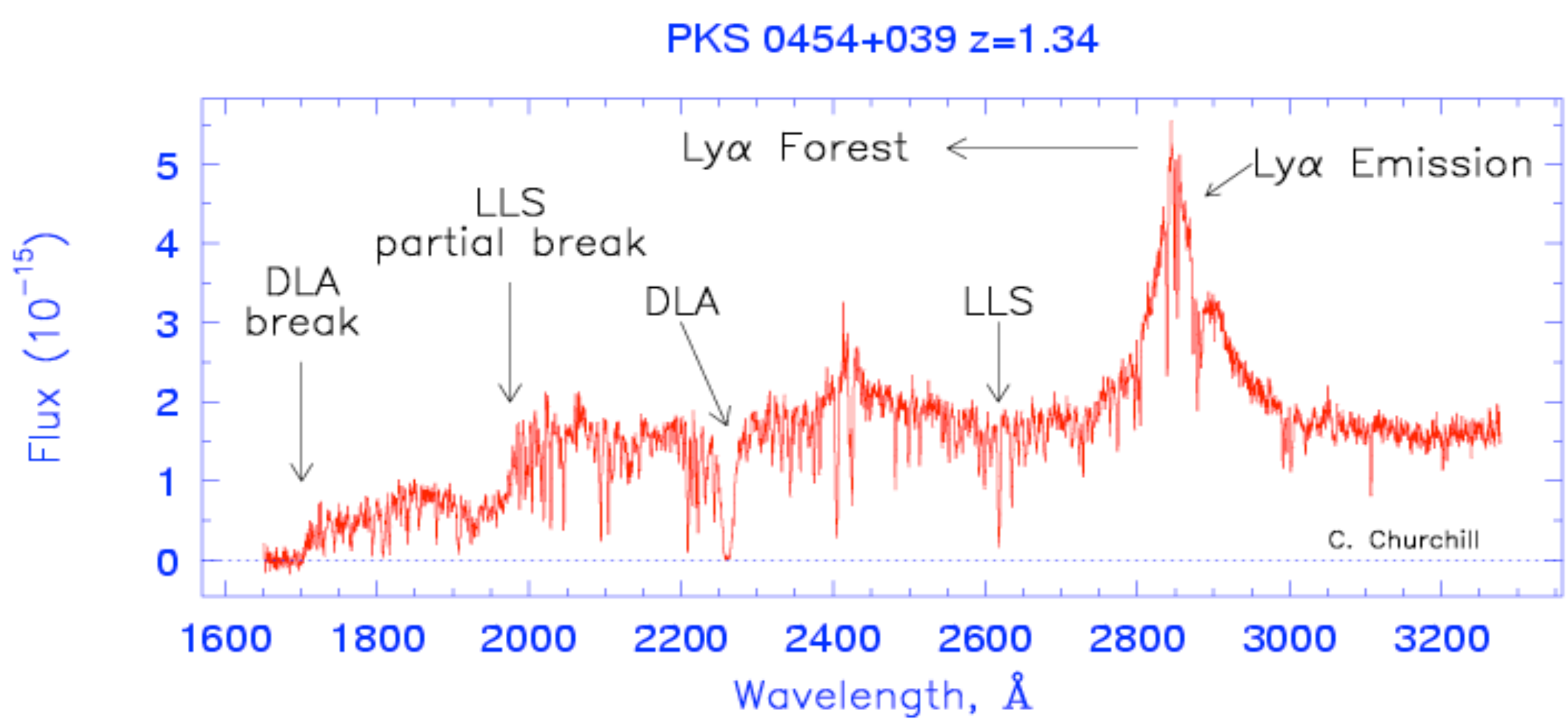

Three main classifications

Lyman-α forest $10^{12} \leq N(HI) \leq 10^{16}$ cm^{-2}

Ly limit systems $10^{18} \leq N(HI) \leq 10^{20}$ cm^{-2}

Damped Lyα $N(HI) \geq 10^{20}$ cm^{-2}

The Lyman-α optical depth from Quasar spectra

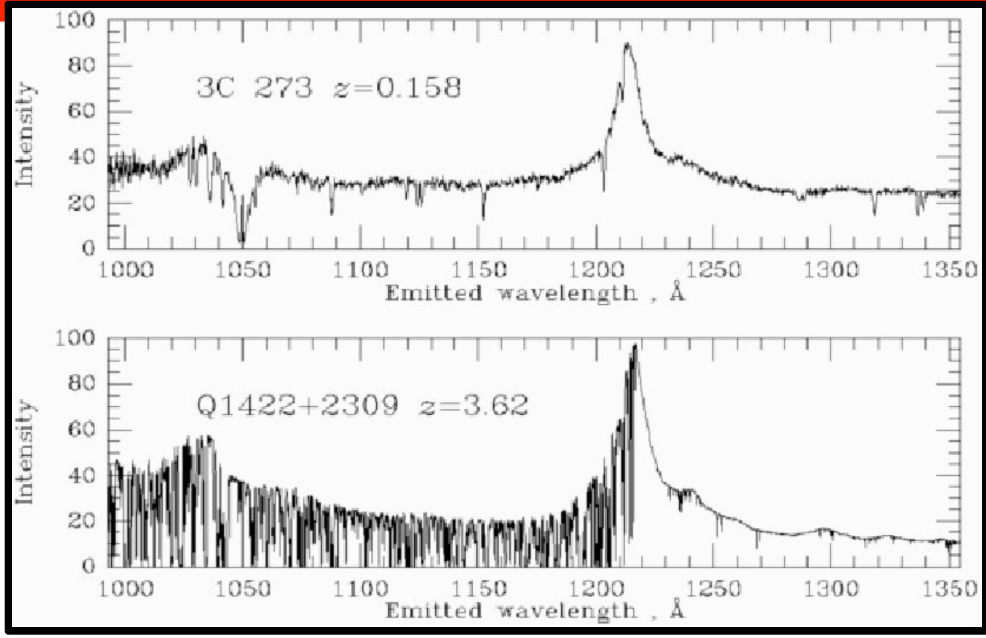

The cross section peaks at the observed frequency:

$$\nu = \nu_0(1+z)\left(1+\frac{v_{pec}}{c}\right)$$

Then substitution in the optical depth (written in terms Redshift) yields:

$$\tau_\alpha = \int n_{HI}\sigma_\alpha(\nu)\frac{cH_o^{-1}dz}{(1+z)\sqrt{\Omega_m(1+z)^3+\Omega_\Lambda}}$$

Which gives the simple result:

$$\frac{n_{HI}}{n_H} = x_{HI} \approx 10^{-4}\Omega_m^{1/2}(1+z)^{\frac{3}{2}}\tau_\alpha$$

The Lyman-α optical depth from Quasar spectra

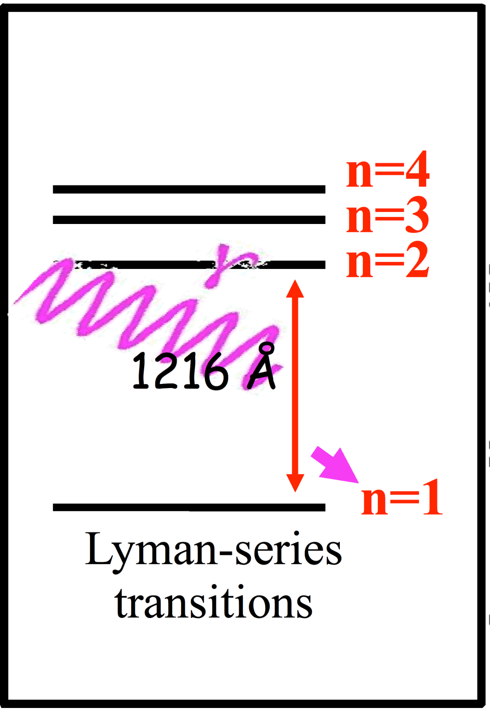

The Lyman-α Forest Along Distant Quasar Spectra ($t_{Universe}$~1 Billion yr)

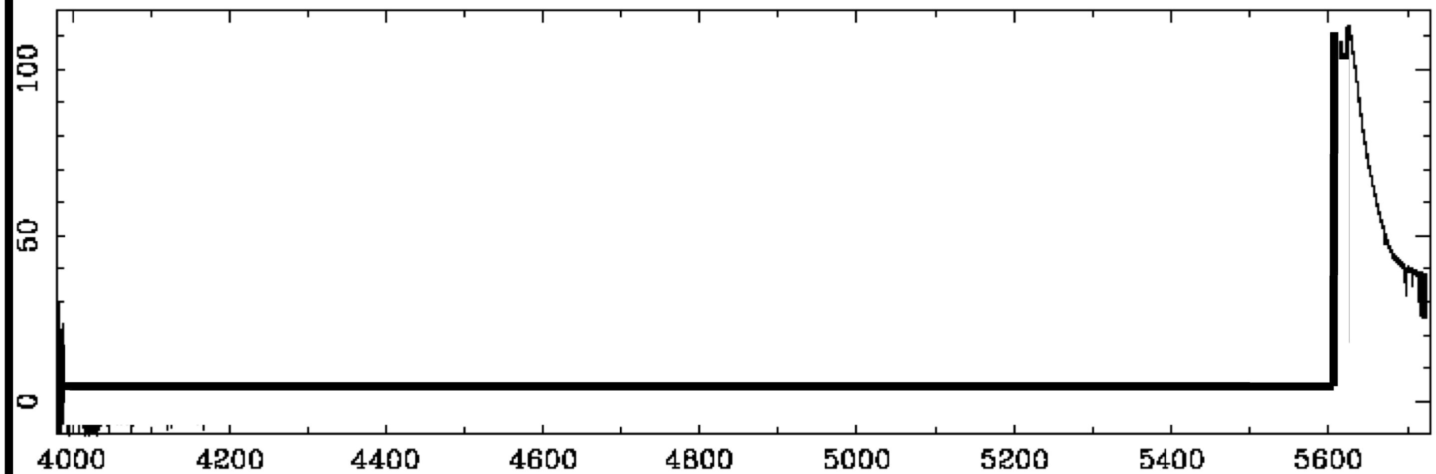

At z ~ 4 the IGM is 10^{-4} neutral

The Lyman-α forest optical depth at z about 6

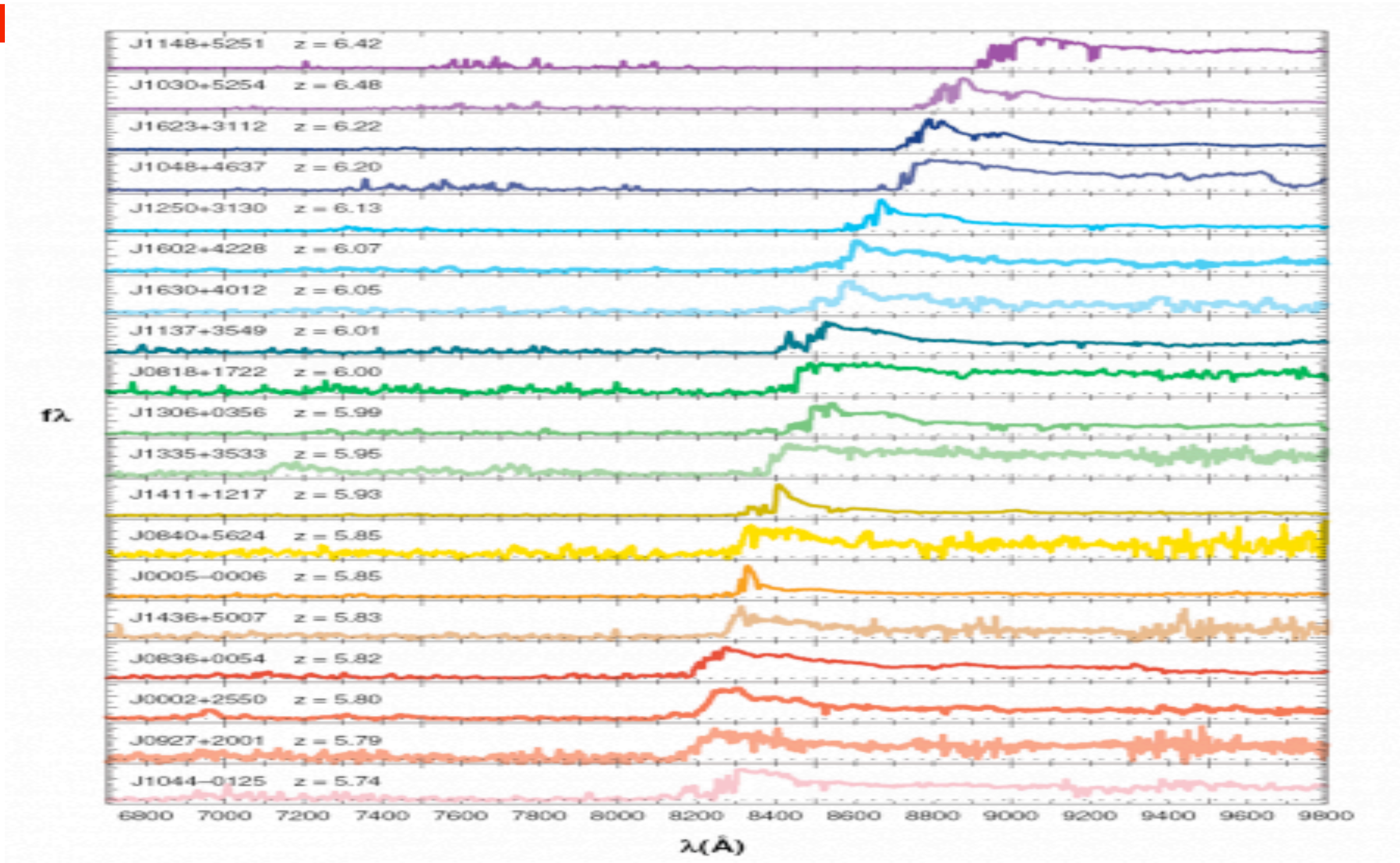

Fan et al. 2003, 2006

The end of the reionization process

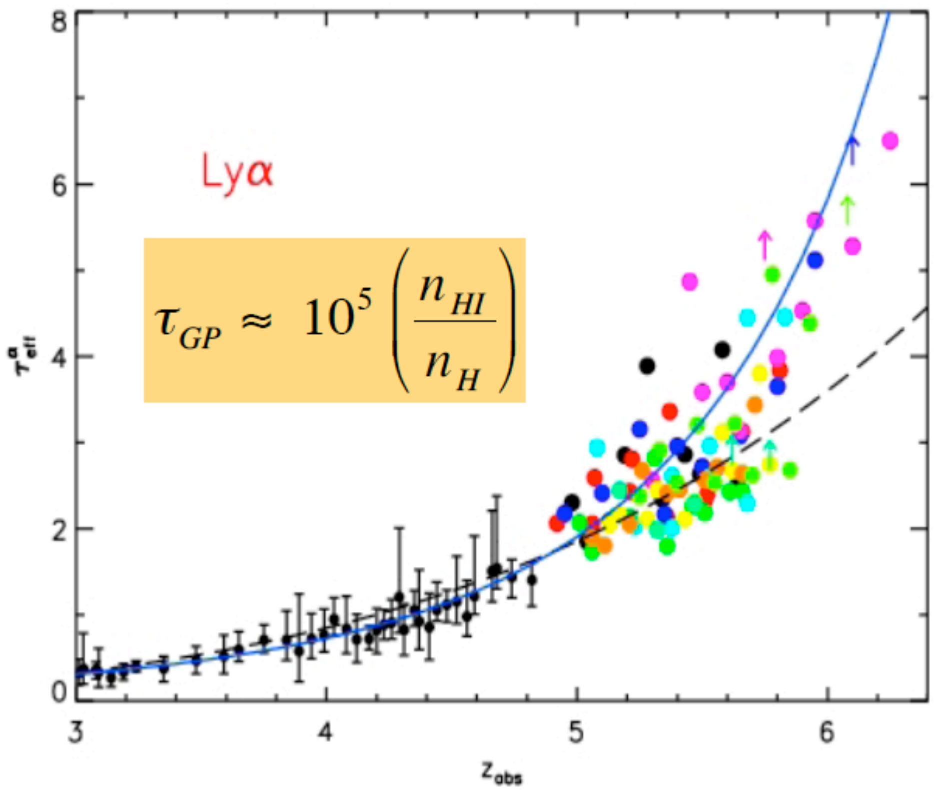

- The Lyman-alpha forest: At z<6 he Universe is completely ionized
- The Universe has completed its ionization by redshift 6: SSDS quasars (however, some, e.g., Mesinger 2009, still claim it is still about 10% neutral)

The IGM Temperature Evolution

Most of the absorption is caused by quasilinear densities that follow a simple equation of state:

$$T = T_0 \left(\frac{\rho}{\bar{\rho}}\right)^{\gamma-1}$$

Since cooling time is long these absorption lines retain information about the thermal history of the IGM

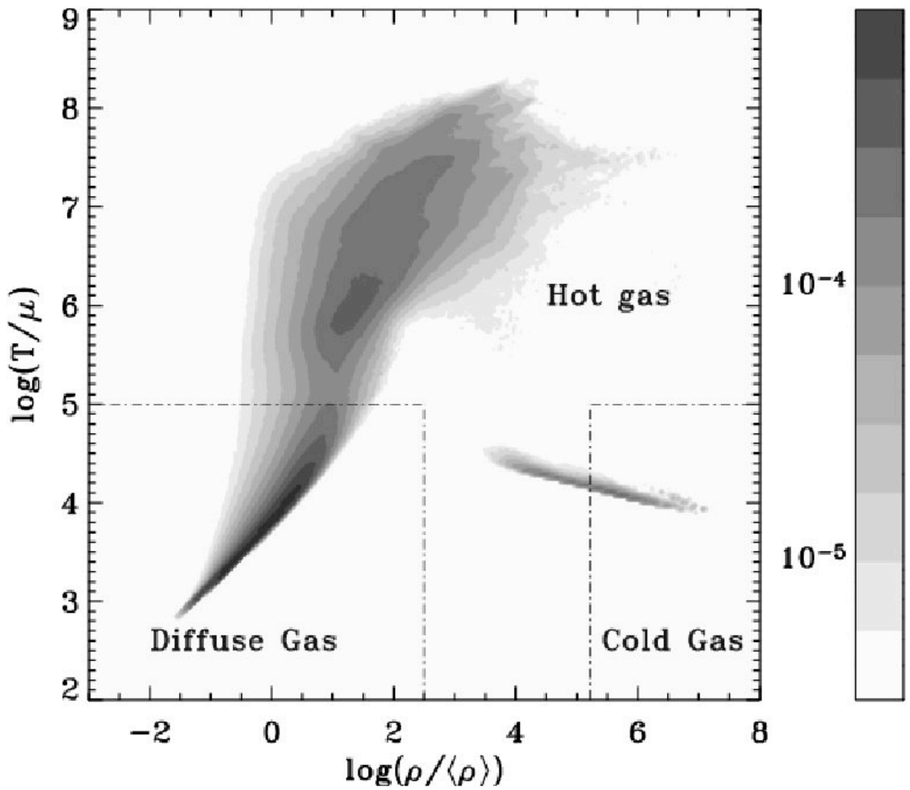

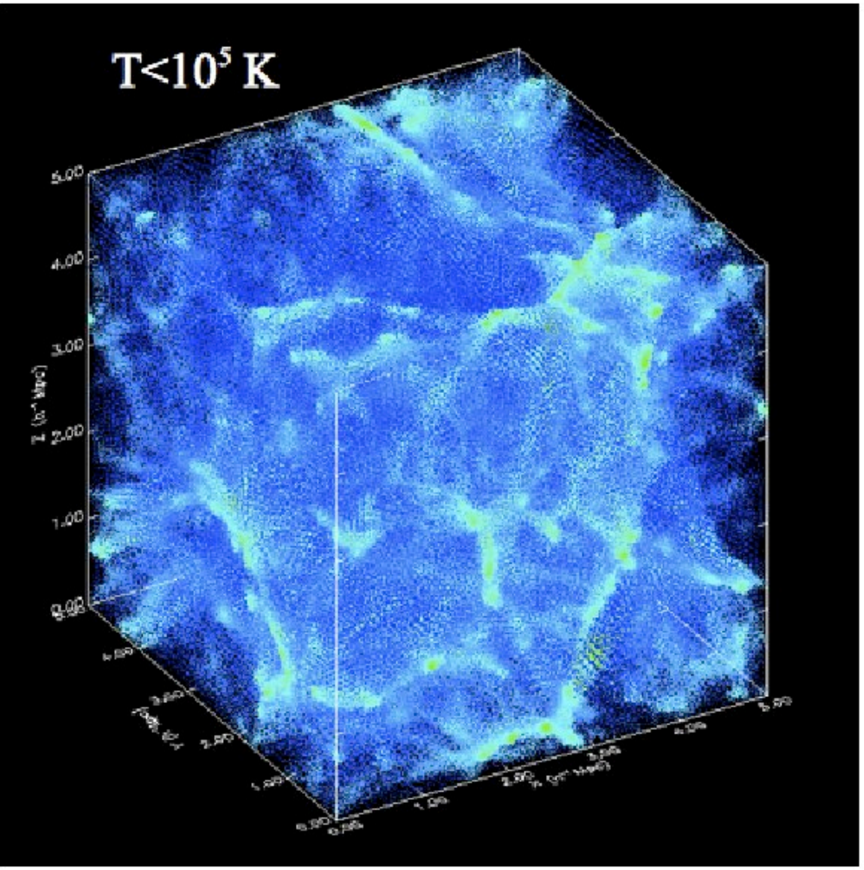

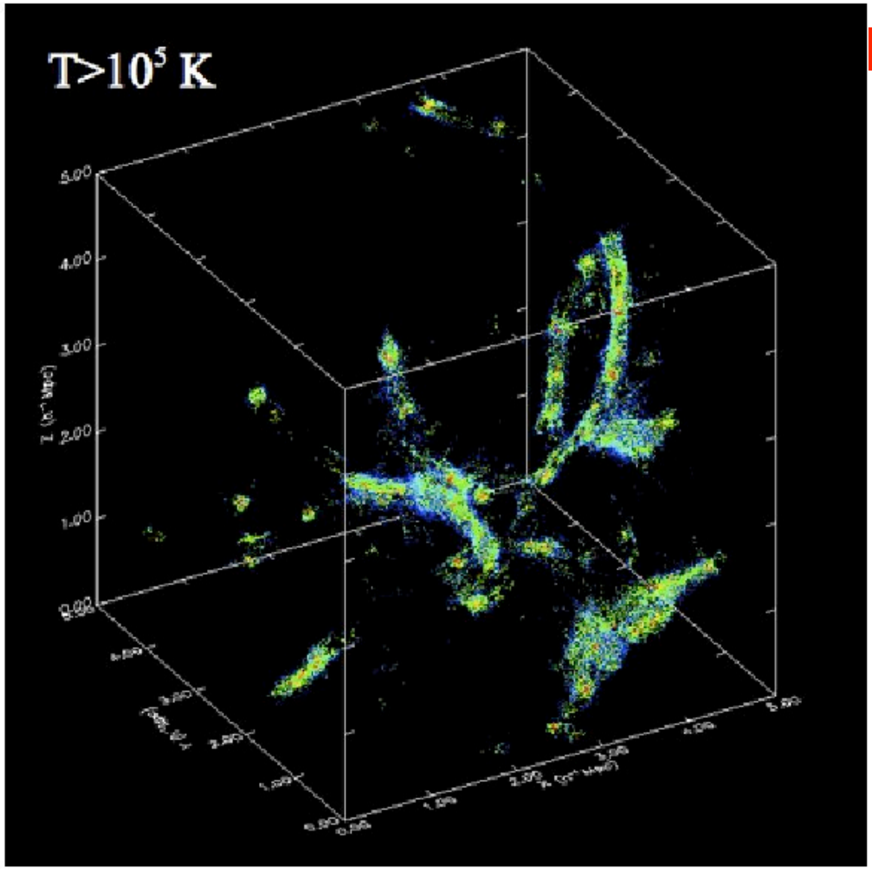

Efstathiou et al 1999

Measurement of IGM Temperature: Wavelet estimate of width of lines

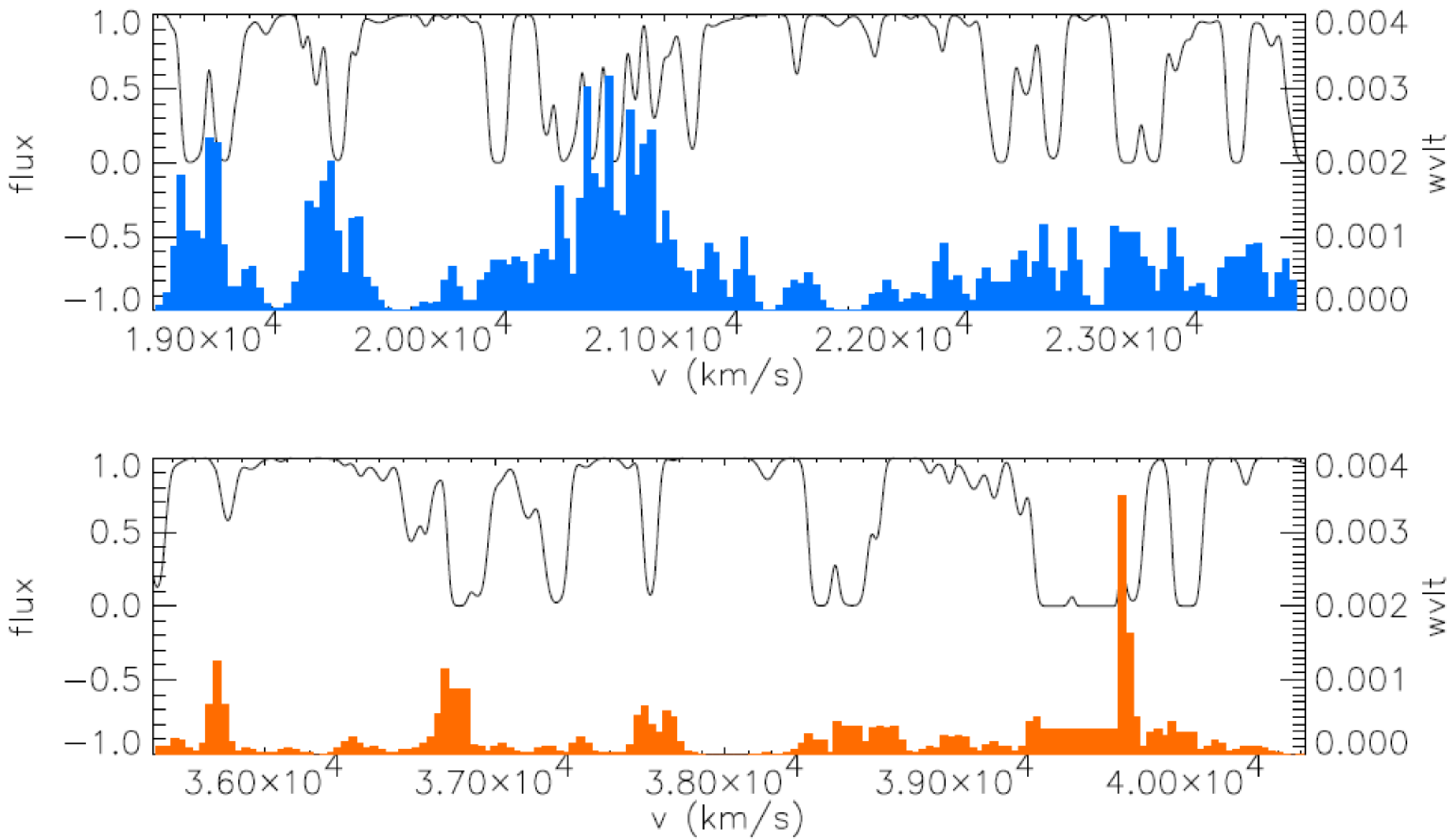

Theuns & Zaroubi 2001

The IGM temperature at low z

$$\frac{1}{T_0}\frac{dT_0}{dt} - \frac{1}{\mu}\frac{d\mu}{dt} = -2H_0 + \frac{\mu\Delta_\epsilon}{-\frac{3}{2}k_B T_0}$$

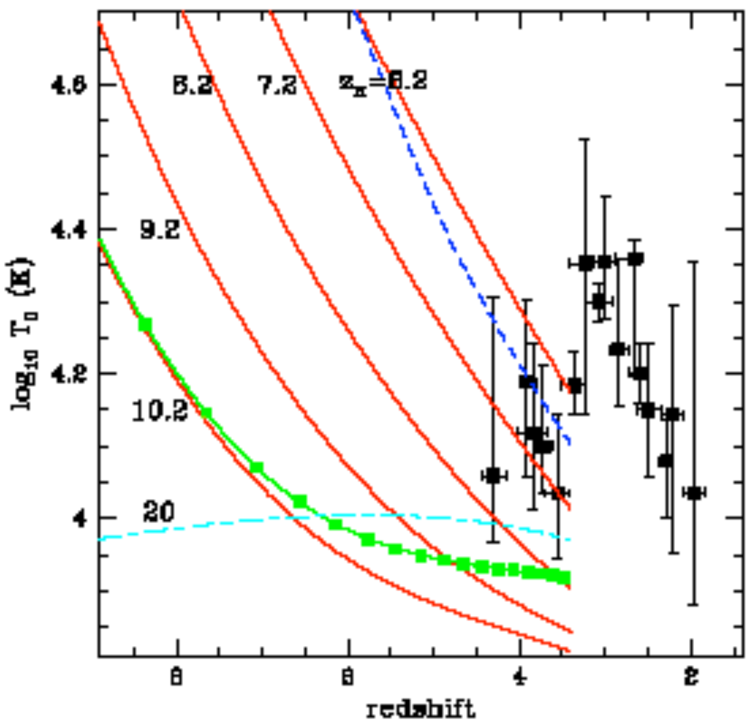

Theuns et al. 2002
Haiman & Hui 2003

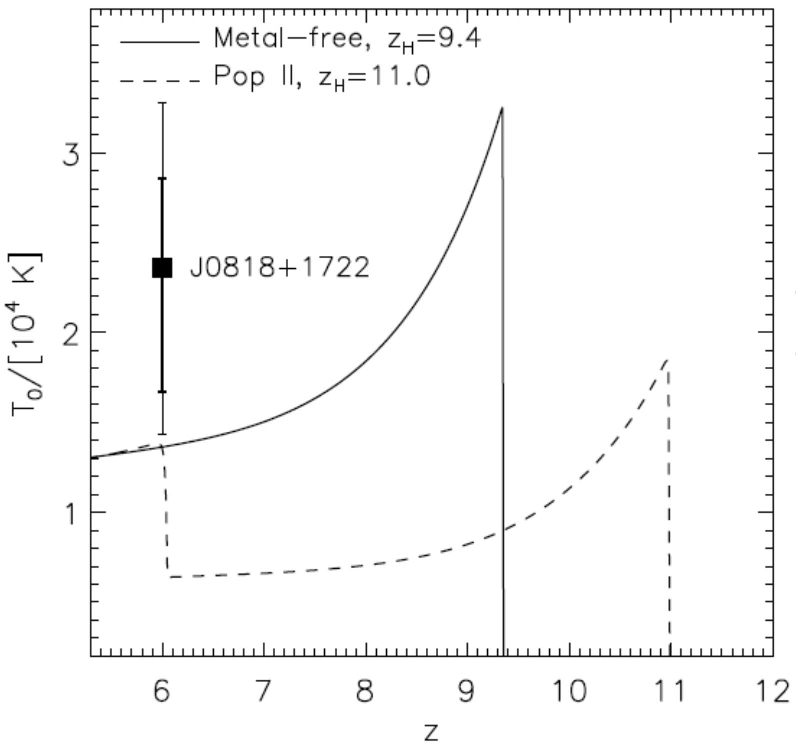

Bolton et al. 2010

Measuring the ionizing emissivity

Galaxy surveys: $\dot{N}_{\rm ion} \propto f_{912/1500} \, \dot{N}_{1500}$

Lyman-α forest opacity: $\dot{N}_{\rm ion} \propto \frac{\Gamma_{\rm ion}}{l_{\rm mfp}}$

Galaxies at z~7-9 HST WPC3 data

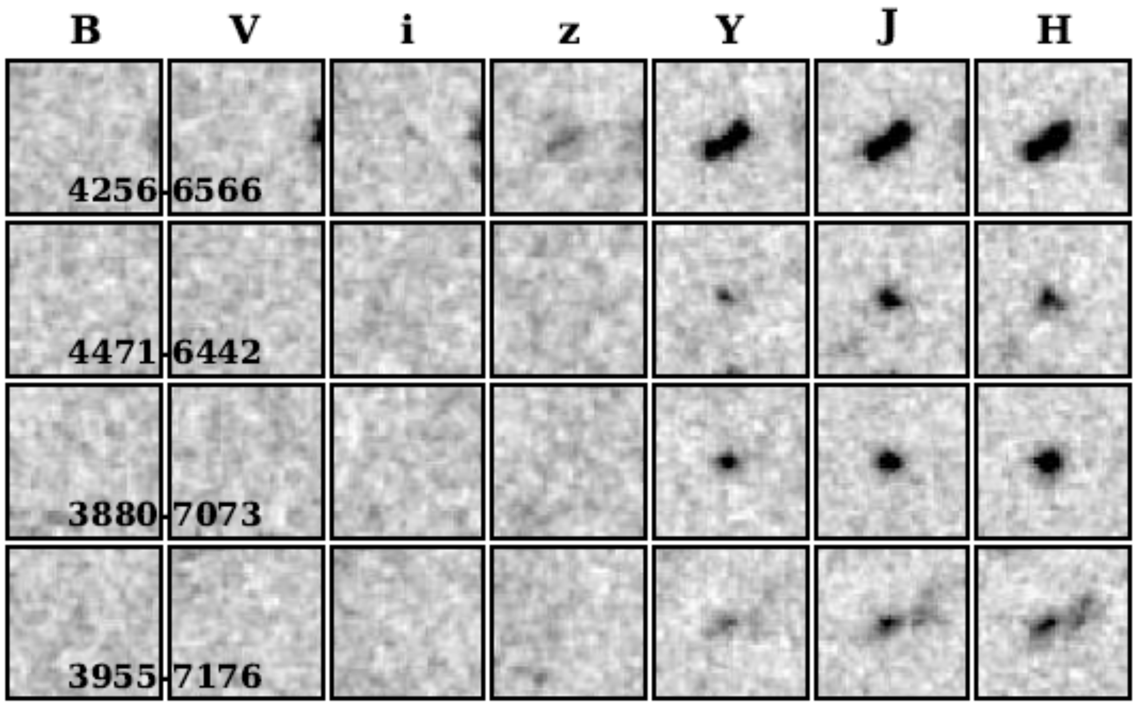

WFC3/IR: 850 - 1170nm
2.1 × 2.3 arcmin field of view
0.13 arcsec pixel^{-1}
10 times survey power of NIC3

UDF 4.7 arcmin^2
60 orbits in YJH
Reaches m_{AB}~29 (5σ)

Oesch et al 2010
Bouwens et a. 2010

Galaxies

Galaxies appear to become bluer and show more Lyα with decreasing luminosity and increasing redshift.

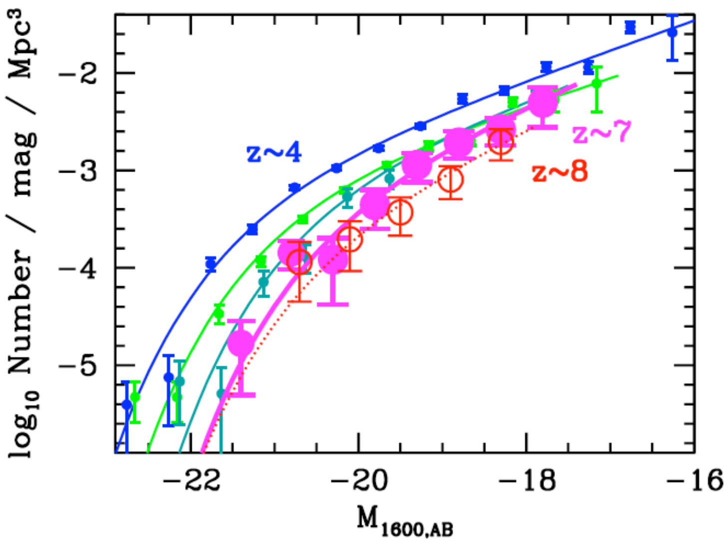

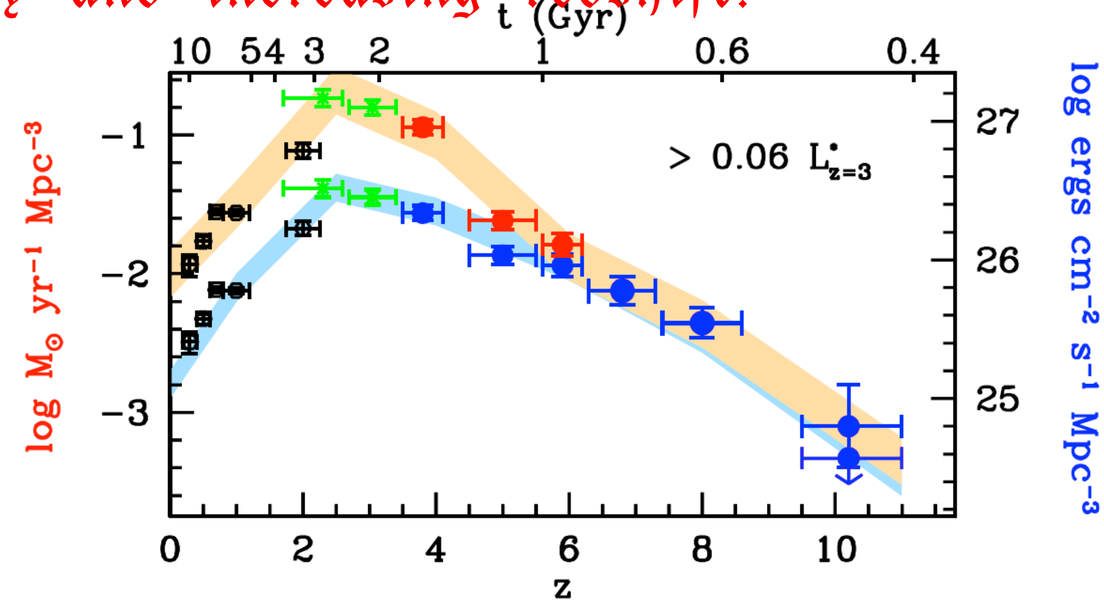

Bouwens et al. 2010

$Z \sim 7$ GALAXIES IN THE HUDF: FIRST EPOCH WFC3/IR RESULTS [1]

P. A. Oesch[2], R. J. Bouwens[3,4], G. D. Illingworth[3], C. M. Carollo[2], M. Franx[4], I. Labbé[5], D. Magee[3], M. Stiavelli[6], M. Trenti[7], P. G. van Dokkum[8]

Draft version December 9, 2009

ABSTRACT

We present a sample of 16 robust $z \sim 7$ z_{850}-drop galaxies detected by the newly installed WFC3/IR camera on the Hubble Space Telescope. Our analysis is based on the first epoch data of the HUDF09 program covering the Hubble Ultra Deep Field with 60 orbits of Y_{105}, J_{125}, and H_{160} observations. These remarkable data cover 4.7 arcmin^2 and are the deepest NIR images ever taken, reaching to ~ 29 mag AB (5σ). The 16 $z \sim 6.5-7.5$ galaxies have been identified based on the Lyman Break technique utilizing $(z_{850} - Y_{105})$ vs. $(Y_{105} - J_{125})$ colors. They have magnitudes $J_{125}= 26.0 - 29.0$ (AB), an average apparent half-light radius of ~ 0.16 arcsec ($\lesssim 1$ kpc), and show very blue colors (some even $\beta \lesssim -2.5$), in particular at low luminosities. The WFC3/IR data confirms previous NICMOS detections indicating that the dropout selection at $z \sim 7$ is very reliable. Our data allow a first determination of the faint end slope of the $z \sim 7$ luminosity function, reaching down to $M_{UV} \sim -18$, a full magnitude fainter than previous measurements. When fixing $\phi_* = 1.4 \times 10^{-3}$ Mpc^{-3}mag^{-1} to the value previously measured at $z \sim 6$, we find a best-fit value of $\alpha = -1.77 \pm 0.20$, with a characteristic luminosity of $M_* = -19.91 \pm 0.09$. This steep slope is similar to what is seen at $z \sim 2-6$ and indicates that low luminosity galaxies could potentially provide adequate flux to reionize the universe. The remarkable depth and resolution of these new images provide insights into the coming power of JWST.

Subject headings: galaxies: evolution — galaxies: high-redshift — galaxies: luminosity function

The Contribution of High Redshift Galaxies to Cosmic Reionization: New Results from Deep WFC3 Imaging of the *Hubble* Ultra Deep Field

Andrew J. Bunker[1], Stephen Wilkins[1], Richard S. Ellis[2],
Daniel Stark[3], Silvio Lorenzoni[1], Kuenley Chiu[2], Mark Lacy[4]
Matt J. Jarvis[5] & Samantha Hickey[5]

ABSTRACT

We have searched for star-forming galaxies at $z \approx 7-10$ by applying the Lyman-break technique to newly-released Y-, J- & H-band images ($1.1, 1.25, 1.6\,\mu$m) from WFC3 on the *Hubble* Space Telescope. By comparing these images of the *Hubble* Ultra Deep Field with the ACS z'-band ($0.85\,\mu$m) images, we identify objects with red colours, $(z'-Y)_{AB} > 1.3$, consistent with the Lyman-α forest absorption at $z \approx 6.7-8.8$. We identify 12 of these z'-drops down to a limiting magnitude $Y_{AB} < 28.5$ (equivalent to a star formation rate of $1.3\,M_{\odot}\,yr^{-1}$ at $z = 7.1$), all of which are undetected in the other ACS filters. We use the WFC3 J-band image to eliminate contaminant low mass Galactic stars, which typically have redder colours than $z \approx 7$ galaxies. One of our z'-drops is a probably a T-dwarf star. The $z \approx 7$ z'-drops appear to have much bluer spectral slopes than Lyman-break galaxies at lower redshift. Our brightest z'-drop is not present in the NICMOS J-band image of the same field taken 5 years before, and is a possible transient object. From the 10 remaining $z \approx 7$ candidates we determine a lower limit on the star formation rate density of $0.0017\,M_{\odot}\,yr^{-1}\,Mpc^{-3}$ for a Salpeter initial mass function, which rises to $0.0025-0.004\,M_{\odot}\,yr^{-1}\,Mpc^{-3}$ after correction for luminosity bias. The star formation rate density is a factor of ≈ 10

We find no robust J-drop candidates at $z \approx 10$. While based on a single deep field, our results suggest that this star formation rate density would produce insufficient Lyman continuum photons to reionize the Universe unless the escape fraction of these photons is extremely high ($f_{esc} > 0.5$), and the clumping factor of the Universe is low.

Even then, we need to invoke a large contribution from galaxies below our detection limit (a steep faint end slope). The apparent shortfall in ionizing photons might be alleviated if stellar populations at high redshift are low metallicity or have a top-heavy initial mass function.

Opacity of the IGM: Photon starved reionization

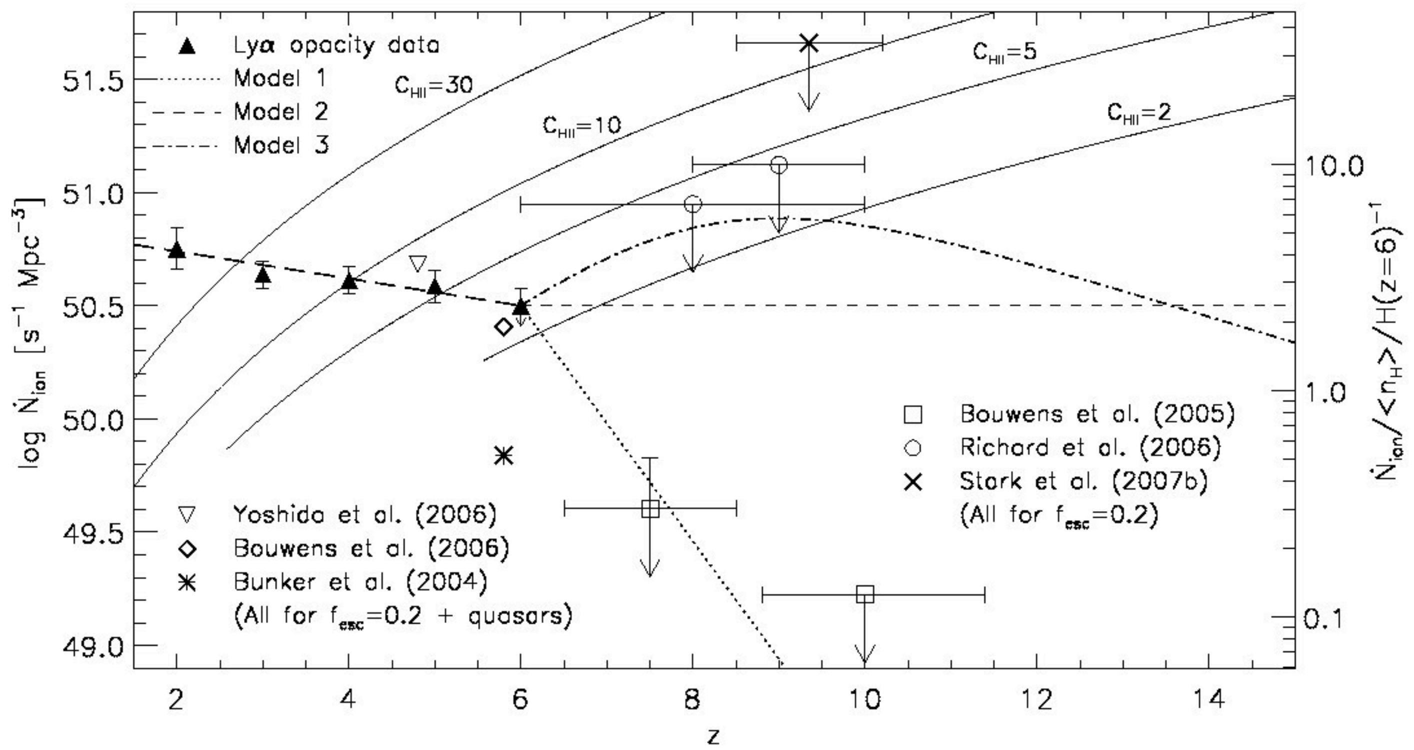

Bolton & Haehnelt 2007

Are we missing photons?

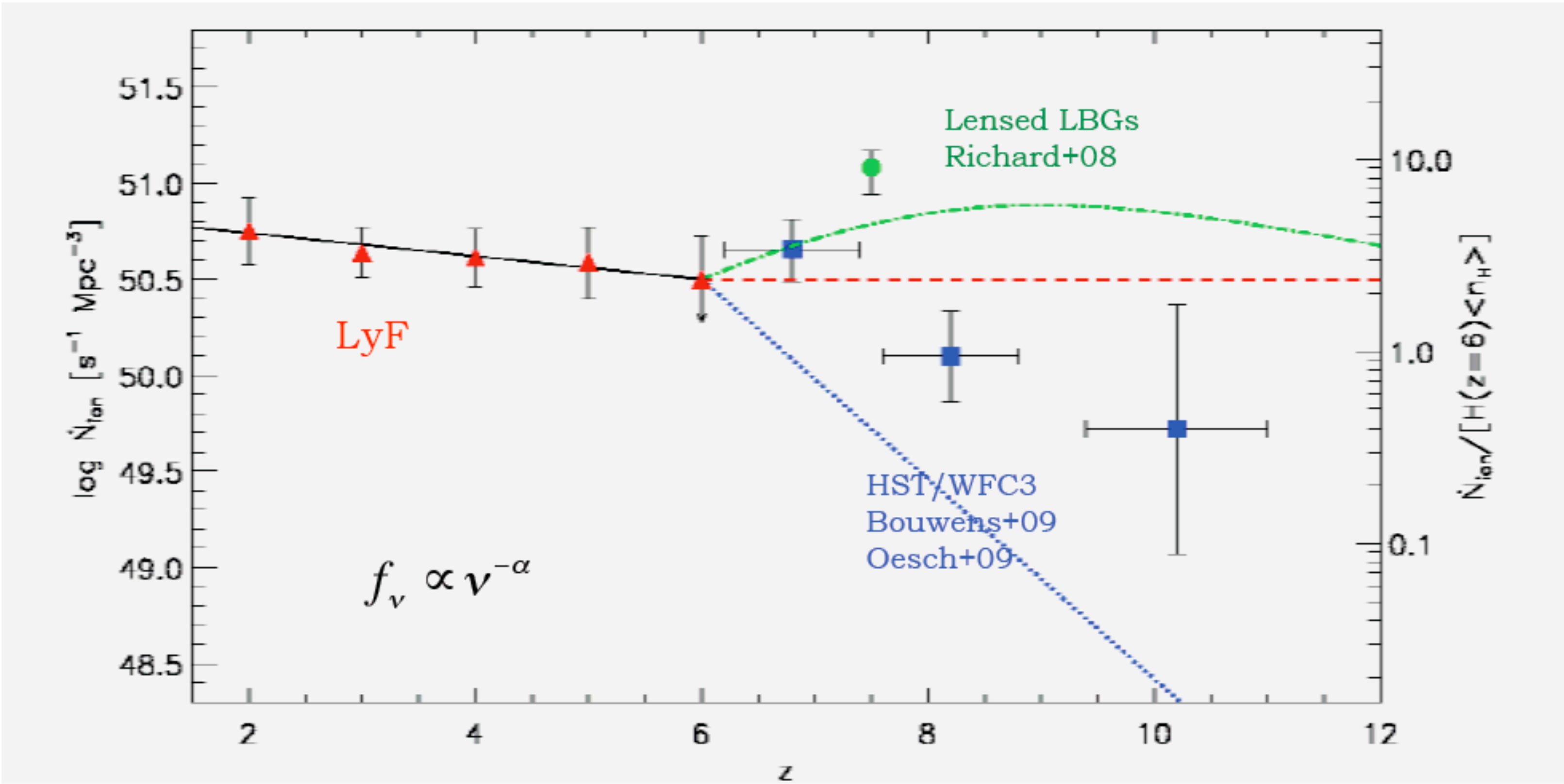

Courtesy of M. Haehnelt

Lyman-α emitters

Lya Luminosity Function (Lya LF)

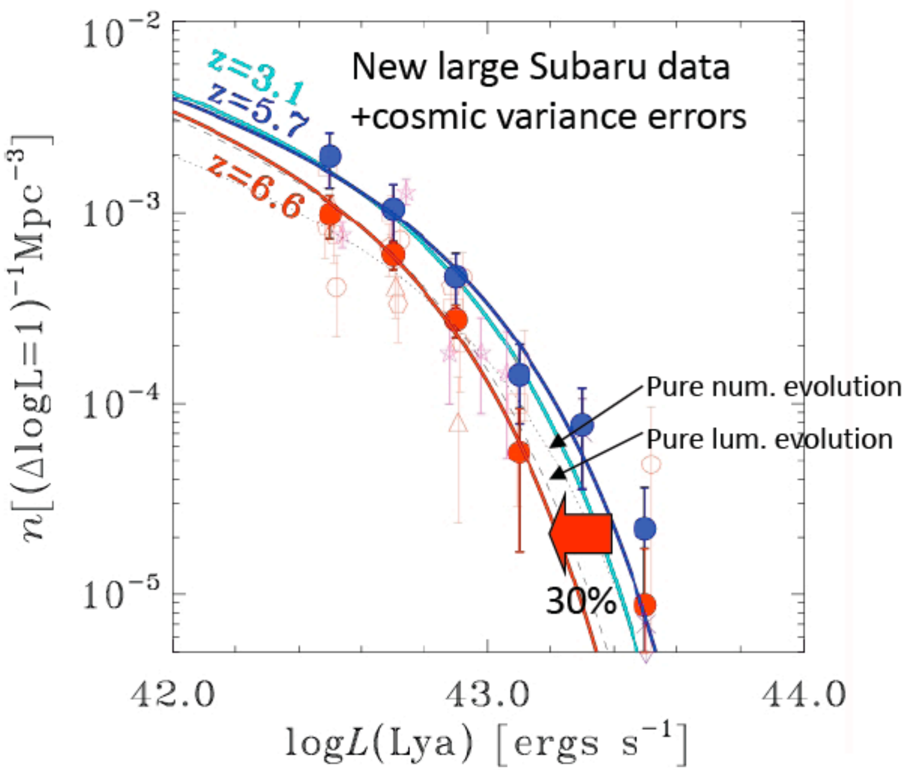

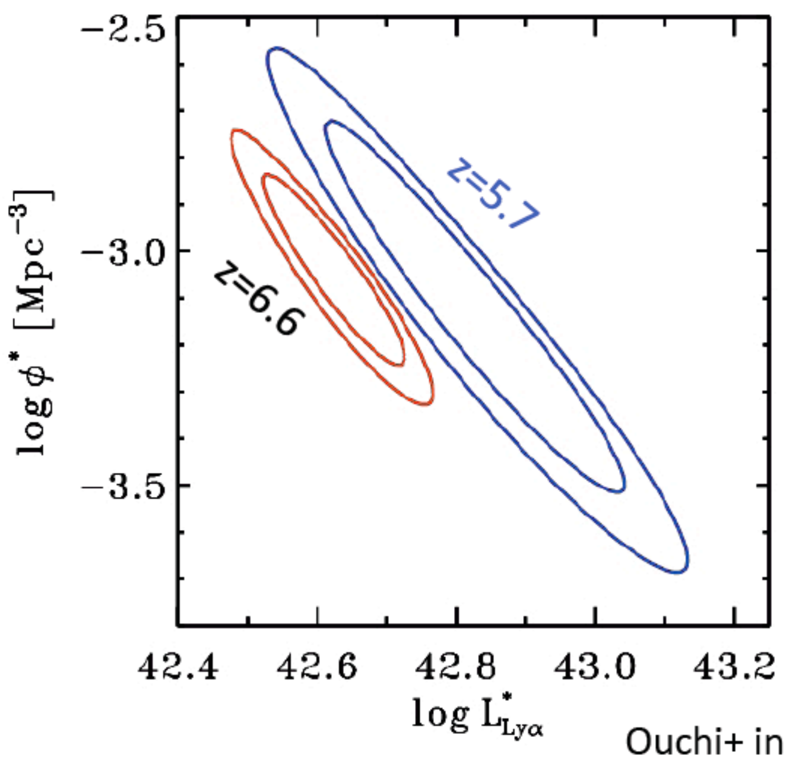

Ouchi+ in prep

Other probe

- Soft x-ray background: constrains ionization by (mini-)QSOs (weak)
- IR background: constrains star light from reionization (unclear results)
- HESS Blazars constrain IR background, gives too little BG (model dependent)
- ......

Summary

- CMB and Lyman-α forest data give the strongest constraints but give no detailed evolution.
- Current observations indicate too few photons per baryon and even those could not be accounted for by high z galaxies. But this is still the beginning.
- Many probes of the EoR but most are indirect and/or model dependent.

We need data from the redshifted 21cm line, which is the most direct probes of reionization.

See lecture tomorrow!